Monodispersed Carbon Nanodots Spontaneously Separated from Combustion Soot with Excitation-independent Photoluminescence

Hao Zhang,[a,b] Junting liang,[c] Jun Liu,*[a] Shaopeng Chen,[c] Hemin Zhang,[a] Zhenfei Tian,[a] Yunyu Cai,[a] Panpan Wang,[a] Yixing Ye[a] and Changhao Liang*[a,b]

We present a facile, low-cost procedure by simple one-step combustion of small organic molecules to obtain ultrafine, hydrophobic, and fluorescent carbon nanodots (CNDs). Without further centrifugation and dialysis, we could easily separate CNDs from combustion soot through spontaneous sedimentation. Transmission electron microscopy and photoluminescence characterization demonstrated that the collected CNDs possessed a monodispersed size distribution with a diameter of 1.9 ± 0.5 nm and excitation-independent luminescent properties. Furthermore, after oxidization treatment, the oxidized CNDs displayed good water solubility and the highest fluorescent intensity at neutral solution.

Introduction

Carbon nanodots (CNDs) are promising candidates in bio-applications because of their optical stability, biocompatibility, and low toxicity.[1–7] Various procedures have been attempted to achieve facile synthesis of CNDs; these procedures can generally be classified into chemical and physical methods.[8] Chemical processes include typical carbon-precursor carbonization,[9–13] solvothermal method,[14,15] and electro-chemical synthesis,[16,17] which can produce high-quality, size-controlled, and functionalized CNDs. However, these methods usually use concentrated acids, strong oxidizing agents, and long purification periods. Physical methods include arc-discharge,[18] laser ablation,[19–21] and plasma treatment.[22,23] These methods can avoid the drawbacks of chemical methods, but they need expensive apparatus and the yield of products is low.

Among the abovementioned methods, the derivation of CNDs from carbon soot is a relatively simple route with high efficiency. For example, Liu et al. synthesized multicolor fluorescent carbon particles through oxidant acid treatment of candle soot followed by centrifugation and dialysis purification processes.[4] More recently, Ko and co-workers used tire soot as raw materials and reported a successful synthesis method for near-infrared fluorescence CNDs (diameter, 11 ± 3 nm).[6] However, in these approaches, the preparation of CNDs from combustion soot requires further treatment, such as thermal refluxing in acid, dialysis, or electrophoresis. Therefore, seeking a more facile and rapid method to obtain ultrafine CNDs with excellent luminescent properties remains a great challenge.

In this paper, we present a facile and rapid combustion approach to prepare CNDs. By simple combustion of small organic molecules (e.g., 1-octene), we obtained ultrafine, monodispersed, hydrophobic, and fluorescent CNDs from combustion soot without further centrifugation and dialysis. Interestingly, such CNDs exhibited excitation-independent photoluminescence (PL). Moreover, these hydrophobic CNDs could easily be transformed to hydrophilic ones via oxidation of H_2O_2.

Experimental

Materials

1-octene (99%) was procured from J&K Scientific. Ethanol (≥99.7%), hydrogen peroxide (H_2O_2, ≥30%), and all other chemicals were purchased from the Sinopharm Chemical Reagent Co., Ltd. All chemicals were used as received without further purification. Ultra-pure water was prepared using a Milli-Q-Plus system.

The synthesis of the CNDs and the oxidized CNDs

CNDs were prepared by burning 1-octene (C_8H_{16}) in air. For safety, a biphase octene–water system was used during combustion. The synthesis process is illustrated in Fig. 1(a–e). Combustion soot was collected at position A and B of the flame and named sample A and B, respectively, as described in Fig. 1(f). Sample A and B could be dispersed in organic polar solvents, such as ethanol, acetone, acetic acid, and chloroform. When sample A was dispersed in ethanol, large particles spontaneously aggregated and completely precipitated in 24 h, and a supernatant bright-yellow solution was observed in the right bottle of Fig. 1(e). However, when sample B was dispersed in ethanol, the suspension was stable for at least one month as shown in the left bottle of Fig. 1(e).

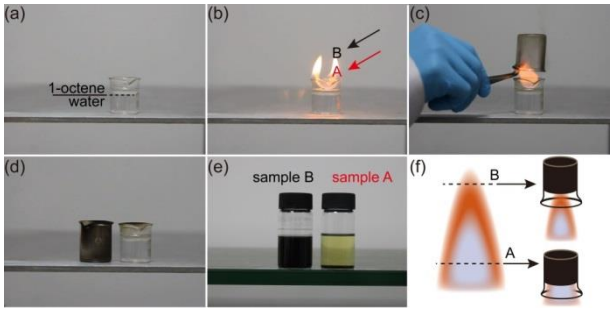

Fig. 1 (a–e) Simple combustion of 1-octene for monodispersed, ultrafine CNDs. (f) Illustration of collecting sites for sample A and B.

The surface of as-prepared CNDs in sample A was hydrophobic, which limited their practical bio-application. Therefore, to make the prepared CNDs hydrophilic, 1.0 mL of 30% H_2O_2 aqueous solution was added to 2.0 mL of the CND colloidal solution. The mixture was dried at 70 ℃–90 ℃ in a vacuum drying oven. Oxidized CNDs (OCNDs) were then obtained, which demonstrated good solubility in water.

Characterizations

The structure and size distribution of CNDs were investigated by transmission electron microscopy (TEM; JEOL JEM-2010, Japan). A MALVERN instrument (Zetasizer 3000 HSa) was used to measure the zeta potential of the suspension of combustion soot. PL measurements were performed with a fluorescence spectrophotometer (F-4600, Hitachi). The compositional analysis of CNDs and OCNDs was performed on X-ray photoelectron spectroscope (ESCALAB 250). The Fourier-transform infrared (FTIR) spectra were recorded with a FTIR apparatus (Nicolet 8700). The pH of OCND aqueous solution was varied by dropwise addition of HCl or NaOH aqueous solution and monitored with a S220 Seven Compact pH meter (Mettler Toledo).

Quantum yield measurements

Quinine sulfate in 0.1 M H_2SO_4 (quantum yield (QY) = 0.54) was chosen as the reference standard. The absolute values were calculated with a standard reference sample that had a fixed and known fluorescence QY, according to the following equation (1):

$$Q = Q_R \frac{I}{I_R} \frac{OD_R}{OD} \frac{n^2}{n_R^2} \quad . \qquad (1)$$

where Q is the QY, I is the measured integrated emission intensity, n is the refractive index, and OD is the optical density. The subscript R refers to the reference fluorophore of known QY.

Cell imaging

Human lung cancer A549 cells were grown in Dulbecco's modified Eagle's medium (DMEM, Hyclone), supplemented with 10% (vol/vol) fetal bovine serum (FBS, Biowest). The cells were maintained in a humidified atmosphere with 5% CO_2 at 37 ℃. Initially, cells were seeded into 12-well plate for 24 h with 60-70% confluent. Then, the cells were cultured in DMEM medium of OCNDs with different concentrations (0–50 mg/L). And the cells were further incubated for 24 h at 37 ℃ in 5% CO_2. Thereafter, the medium was removed and the cells were washed with Phosphate Buffered Saline three times. Finally, the cells were photographed by a fluorescence microscope (Olympus) with excitation filters for UV.

Results and discussion

The TEM image of the product from supernatant solution in sample A is shown in Fig. 2(a). The CNDs were clearly uniform in size with good dispersion. The size distribution of CNDs was determined from the statistical analysis of 300 nanoparticles based on TEM images. The corresponding size distribution histogram in Fig. 2(b) indicated that the CNDs were monodispersed with an average size of 1.9 ±0.5 nm. This size distribution was much more uniform and smaller than that of previously reported CNDs derived from combustion soot.[24] The HRTEM image (inset at the upright corner of Fig. 2(a)) indicated the crystalline nature of CNDs with a lattice spacing of 0.24 nm.

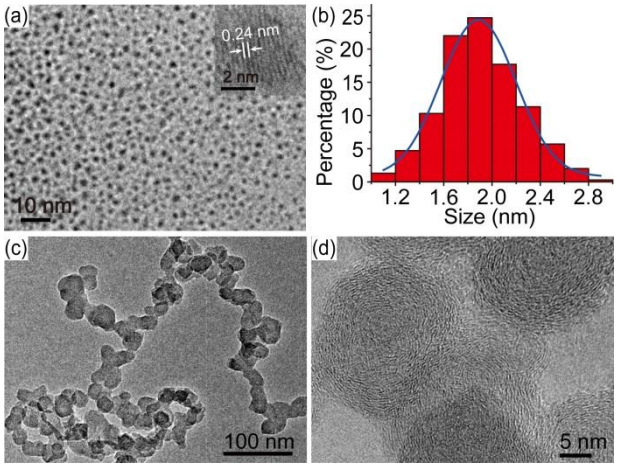

Fig. 2 (a) TEM image and (b) size histogram of the CNDs obtained in sample A (inset shows HRTEM image of a single CND). TEM (c) and HRTEM (d) image of carbon products in sample B.

Fig. 2(c) and (d) show typical TEM images of the product formed in sample B. Onion-like carbon nanoparticles with a size of ~22 nm were observed, and no fine CNDs were found. CNDs could not be obtained from the combustion soot collected at the top position of the combusting flame. These results demonstrated that the collection position of combustion soot in flame was critical to the carbon product. The disappearance of CNDs in sample B was probably due to the further growth and attachment of CNDs in flame.[25,26] Dobbins et al. also proved that the size of particles from the centerline of the flame increases with the height above the bottom of the flame.[27] Therefore, CNDs could be collected at the position in the inner flame by combustion of small organic molecules.

According to the experimental observation, we found that the CNDs could be separated spontaneously from sample A in ethanol solution without further purification, such as centrifugation, dialysis, or electrophoresis. The reason for the spontaneous separation of CNDs in sample A was investigated. The chemical ionization reaction was proposed as the mechanism of the formation of combustion soot and charged particles in flame.[25,26,28] Therefore, we inferred that the charged surface of particles in flame was responsible for colloidal stability. Zeta potential is usually used to measure the stability of a colloidal solution, and a high zeta potential results in strong repulsion that prevents aggregation.[29,30] As such, we measured the zeta potentials of sample A and B. As shown in Fig. 3, the zeta potential pattern of sample A and B displayed a positive zeta potential (+18.9 mV) and a negative zeta potential (−54.2 mV), respectively. According to the literature, colloids are considered to have good stability when characterized by an absolute value of zeta potential within the range of 41–60 mV.[31] However, if the absolute value is below 30 mV, the colloid prefers aggregation and sedimentation.[29] These findings were in agreement with the stability of sample A and B, as shown in Fig. 1(e). Therefore, a low absolute value of zeta potential of combustion soot was the fundamental reason for the spontaneous separation of CNDs in sample A.

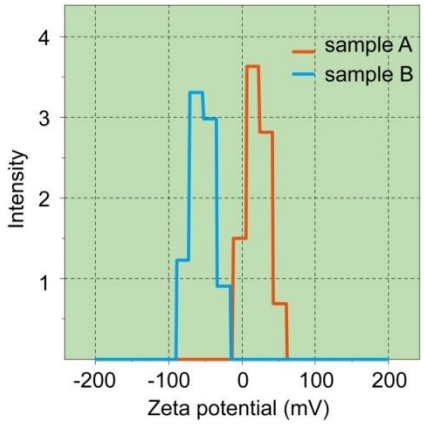

Fig. 3 Zeta potential pattern of sample A (red) and B (blue) dispersed in ethanol.

The optical properties of CNDs dispersed in ethanol were investigated by optical emission spectroscopy. The PL spectra presented three PL peaks centered at 406, 432, and 458 nm (Fig. 4(a)). Interestingly, all the PL peaks did not shift when the excitation wavelength was altered, except for a change in relative intensity. This distinctive excitation-independent PL was different from most excitation-dependent PL reported in previous studies.[8] The PL excitation (PLE) spectra (Fig. 4(b)) were further measured at the detected wavelengths of 406, 432, and 458 nm. Most of the PLE peaks did not notably shift at different emission wavelengths. The calculated PL QY of the CNDs was 14.9% with quinine sulfate used as a reference (Table 1).

Table 1. Quantum yield of CNDs (in absolute ethanol) and OCNDs (in water) using quinine sulfate as a reference.

Sample	Excitation wavelength λ_{ex} (nm)	I	OD	n	Q
Quinine sulfate	306	537918	0.017	1.33	0.54
	320	401605	0.020	1.33	0.54
CNDs	306	326658	0.039	1.36	0.149
OCNDs	320	165641	0.088	1.33	0.051

As described above, both PL and PLE spectra of prepared CNDs displayed multiple peaks, which indicated that multiple energy levels were related to the stimulated emission processes. However, whether these energy levels originate from intrinsic states or defect states was analyzed. As reported in previous studies,[8] defect states usually display luminescence after the blue region and exhibit excitation-dependent emission, which were inconsistent with our results. Thus, we suggested that the distinctive optical properties should arise from intrinsic states. As reported by Radovic et al., the carbon products derived from combustion soot might have carbyne- and/or carbene-like structures, both of which have seven HOMO and LUMO energy levels with two singlet levels and five triplet levels.[32]

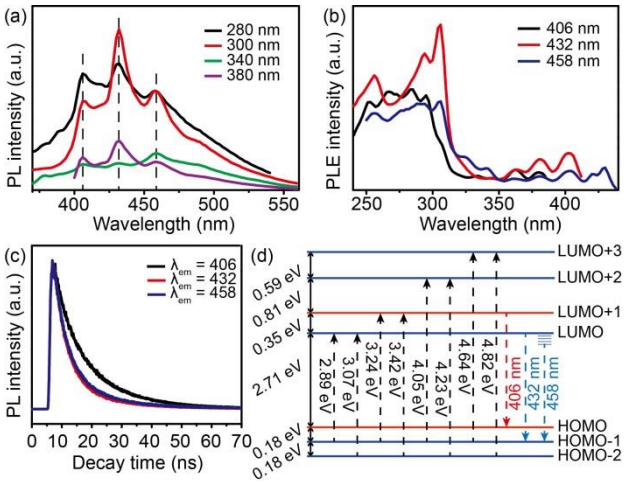

Fig. 4 (a) PL spectra of CNDs excited at 280, 300, 340, and 380 nm. (b) PLE spectra of CNDs at detection wavelengths of 406, 432, and 458 nm. (c) TRPL decay profile of CNDs recorded at different emission wavelengths of 406, 432, and 458 nm. (d). Schematic of the electric structure of CNDs based on PLE data in Fig. 4(b). HOMO and LUMO+1 are singlets, whereas all other values are triplets.

Thus, we speculated the electronic structure (Fig. 4(d)) of CNDs based on PLE spectra. However, singlet/triplet levels are still indistinguishable. Thus, the recombination dynamics of CNDs were investigated, the results showed in Fig. 4(c). It is apparently that decay curves detected at 406 nm (3.05 eV) displayed a longer decay time than those detected at 432 and 458 nm. The difference should be attributed to the delay time of intersystem crossing (10^{-10}-10^{-8} s) between singlet and triplet excited states,[33] and also implies that emission of 406 nm might correspond to radiation transition between singlet levels. But, as shown in Fig. 4(d), the energy gaps from LUMO+1 to HOMO and from LUMO to HOMO-2 are 3.06 eV and 3.07 eV, respectively, which are both very close to 3.05 eV (406 nm). If LUMO is singlet state, radiation transition of the emission of 432 nm (2.87 eV) from LUMO to HOMO-1 will be spin-forbidden transition. It would result in a much longer delay time detected at 432 nm than that detected at 406 nm. Therefore, we can confirm that LUMO+1 and HOMO are singlets, whereas the others are triplets. Since the HOMO is singlet, the luminescence resources reasonably originated from the carbyne-like structure.[22,32]

In addition, as-prepared CNDs are hydrophobic, which limits their practical bio-application. Oxidization treatment is a common method to make CNDs hydrophilic by introducing hydrophilic oxygenous functional groups, such as carboxyl groups, on the surfaces of CNDs.[4] In the present study, we treated CNDs with a certain amount of 30% H_2O_2 and found that the CNDs showed good solubility in water after oxidation. The FTIR spectrum of OCNDs revealed a peak centered at 1735 cm^{-1}, which corresponded to the stretching vibration of C=O bonds in carboxyl groups (Fig. 5a). The carboxyl groups were also confirmed by X-ray photoelectron spectroscopy (XPS) characterizations showed in Fig. 5b. High-resolution XPS spectra of C 1s peaks displayed the presence of C=O bonds (289.1 eV) related to the carboxyl groups, as well as C=C bonds (284.6 eV). Elemental analysis indicated that the oxygen content of OCNDs was 37.27 at.%, while oxygen content of CNDs was only 3.24 at.%. The large increase of oxygen content should be attributed to hydrogen dioxide treatment. However, small amount of oxygen of CNDs might result from the exposure of samples to air.[22] Furthermore, the OCND aqueous solution was acidic, indicating the appearance of carboxyl groups on the surface of OCNDs, which should be responsible for the hydrophilicity of OCNDs.

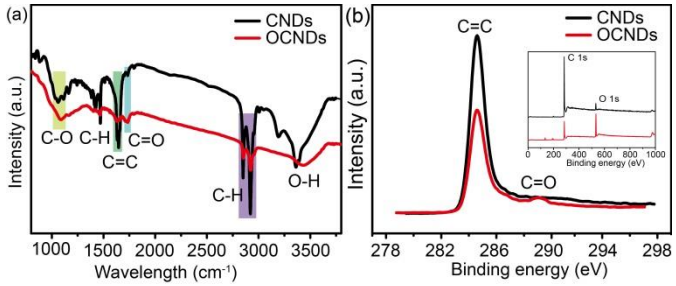

Fig. 5 (a) FTIR spectra of CNDs and OCNDs; (b) High-resolution XPS spectra of C 1s peaks of CNDs and OCNDs. Inset: XPS patterns of CNDs and OCNDs.

The PLE and PL spectra of OCNDs dispersed in water are shown in Fig. 6(a). The PLE spectra presented two peaks centered at 264 and 320 nm at a detection wavelength of 436 nm. The PL peaks exhibited a slight red-shift when the excitation wavelength varied from 300 nm to 370 nm. The QY of the OCNDs was also measured with quinine sulfate as the reference, but the value decreased to 5.1% compared with that of CNDs (Table S1). Except for water solubility, environmental factor is also important to practical bio-applications. Therefore, we investigated PL emission behaviours of the OCNDs under varied pH values (Fig. 6(b)). The highest fluorescent intensity of the OCNDs was observed at neutral condition.

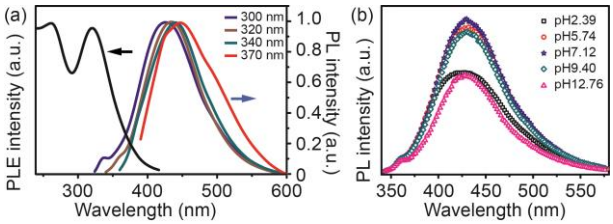

Fig. 6 (a) PLE spectra of OCNDs with an emission wavelength of 436 nm and PL spectra of OCNDs excited at 300, 320, 340, and 370 nm. (b) pH-dependent PL intensity of OCNDs excited at 320 nm.

The fluorescence imaging of OCNDs in Human lung cancer A549 cells was then investigated by fluorescence microscope. The result clearly showed that auto-fluorescence from the cells themselves was undetectable upon UV illumination (Fig 7 (b)). However, bright fluorescence was observed (Fig 7 (d), (f)) from cells incubated with OCNDs. Furthermore, the fluorescence intensity increased significantly with the concentration of OCNDs from 10 mg/L to 50 mg/L. These results indicated that OCNDs could penetrate into the cell easily and accumulate in the cell. Thus, the material of OCNDs provided great promise in serving for cell-imaging applications.

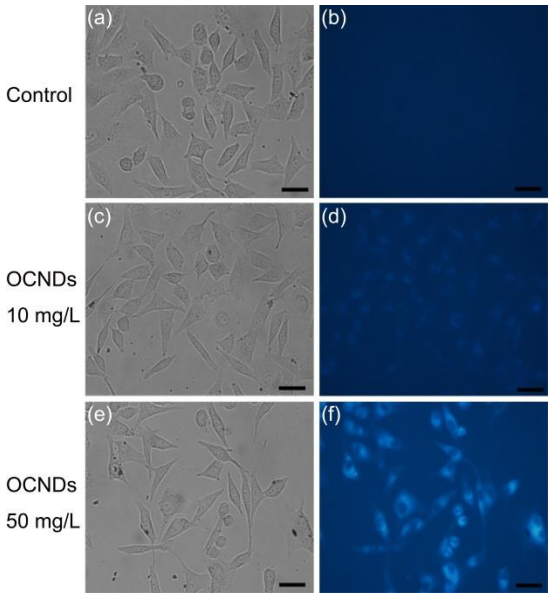

Fig. 7 Representative fluorescence micrograph of A549 cells treated in the absence (control) or presence of the CNDs as described in Methods. Cells untreated (a, b) were no fluorescence while most all of cells were positive (blue) when treated by CNDs at 10 mg/L (c, d) or 50 mg/L (e, f). Scale bar = 1 mm.

Conclusions

We presented a low-cost, one-step approach to obtain ultrafine, monodispersed, and luminescent CNDs by facile combustion of small molecules. Given the small absolute value of zeta potential of large soot particles, CNDs were purified by spontaneous sedimentation. The size distribution of the CNDs was relatively narrow with an average diameter of 1.9 ±0.5 nm. Most interestingly, CNDs, of which the QY was approximately 14.9%, presented special excitation-independent PL features that could be easily distinguished from common excitation-dependent fluorophores. Such CNDs could only be dispersed in polar organic solvents, but oxidization by H2O2 could make them soluble in water. The OCNDs displayed a QY of 5.1% and the highest fluorescent intensity at neutral solution. These OCNDs should have potential applications in bio-imaging and labelling.

Acknowledgement

We thank the financial supports from the National Basic Research Program of China (2014CB931704), the National Natural Science Foundation of China (NSFC, No. 11304315, 11204308, 51401206, 11404338, 51371166) and the CAS/SAFEA International Partnership Program for Creative Research Teams).

Notes and references

1 Q. L. Zhao, Z. L. Zhang, B. H. Huang, J. Peng, M. Zhang and D. W. Pang, *Chem. Commun.*, 2008, **41**, 5116-5118.
2 J. H. Shen, Y. H. Zhu, X. L. Yang, and C. Z. Li, *Chem. Commun.*, 2012, **48**, 3686-3699.
3 R. Q. Ye, C. S. Xiang, J. Lin, Z. W. Peng, K. W. Huang, Z. Yan, N. P. Cook, E. L. G. Samuel, C. C. Hwang, G. Ruan, G. Ceriotti, A. O. Raji, A. A. Martí, and M. Tour, *Nat. Commun.*, 2013, **4**, 2943.
4 H. P. Liu, T. Ye, and C. D. Mao, *Angew. Chem. Int. Ed.*, 2007, **46**, 6473-6475.
5 L. Tian, D. Ghosh, W. Chen, S. Pradhan, X. J. Chang, and S. W. Chen, *Chem. Mater.*, 2009, **21**, 2803-2809.
6 H. Y. Ko, Y. W. Chang, G. Paramasivam, M. S. Jeong, S. Cho, and S. Kim, *Chem. Commun.*, 2013, **49**, 10290-10292.
7 R. J. Fan, Q. Sun, L. Zhang, Y. Zhang, and A. H. Lu, *Carbon*, 2014, **71**, 87-93.
8 H. T. Li, Z. H. Kang, Y. Liu, and S. T. Lee, *J. Mater. Chem.*, 2012, **22**, 24230-24253**.**
9 L. B. Tang, R. B. Ji, X. K. Cao, J. Y. Lin, H. X. Jiang, X. M. Li, K. S. Teng, C. M. Luk, S. J. Zeng, J. H. Hao, and S. P. Lau, *ACS nano*, 2012, **6**, 5102-5110.
10 D. Y. Pan, J. C. Zhang, Z. Li, C. Wu, X. M. Yan, and M. H. Wu, *Chem. Commun.*, 2010, **46**, 3681-3683.
11 R. L. Liu, D. Q. Wu, S. H. Liu, K. Koynov, W. Knoll, and Q. Li, *Angew. Chem. Int. Ed.*, 2009, **121**, 4668-4671.
12 P. Dubey, K. M. Tripathi, and S. K. Sonkar, *RSC Adv.*, 2014, **4**, 5838-5844.
13 K. M. Tripathi, A. K. Sonker, S. K. Sonkar, and S. Sarkar, *RSC Adv.*, 2014, **4**, 30100-30107.
14 S. J. Zhu, J. H. Zhang, C. Y. Qiao, S. J. Tang, Y. F. Li, W. J. Yuan, B. Li, L. Tian, F. Liu, R. Hu, H. N. Gao, H. T. Wei, H. Zhang, H. C. Sun, and B. Yang, *Chem. Commun.*, 2011, **47**, 6858-6860.
15 D. Y. Pan, J. C. Zhang, Z. Li, and M. H. Wu, *Adv. Mater.*, 2010, **22**, 734-738.
16 H. T. Li, X. D. He, Z. H. Kang, H. Huang, Y. Liu, J. L. Liu, S. Y. Lian, C. H. A. Tsang, X. B. Yang, and S. T. Lee, *Angew. Chem. Int. Ed.*, 2010, **49**, 4430-4434.
17 Y. Li, Y. Hu, Y. Zhao, G. Q. Shi, L. Deng, Y. B. Hou, and L. T. Qu, *Adv. Mater.*, 2011, **23**, 776-780.
18 X. Y. Xu, R. Ray, Y. L Gu, H. J. Ploehn, L. Gearheart, K. Raker, and W. A. Scrivens, *J. Am. Chem. Soc.*, 2004, **126**, 12736-12737.
19 S. L. Hu, K. Y. Niu, J. Sun, J. Yang, N. Q. Zhao, and X. W. Du, *J. Mater. Chem.*, 2009, **19**, 484-488.
20 X. Y. Li, H. H. Wang, Y. Shimizu, A. Pyatenko, K. Kawaguchi, and N. Koshizaki, *Chem. Commun.*, 2010, **47**, 932-934.
21 Y. P. Sun, B. Zhou, Y. Lin, W. Wang, K. A. S. Fernando, P. Pathak, M. J. Meziani, B. A. Harruff, X. Wang, H. F. Wang, P. G. Luo, H. Yang, M. E. Kose, B. Chen, L. M. Veca, and S. Y. Xie, *J. Am. Chem. Soc.*, 2006, **128**, 7756-7757.
22 J. Kim, and J. S. Suh, *ACS nano*, 2014, **8**, 4190-4196.
23 H. Q. Jiang, F. Chen, M. G. Lagally, and F. S. Denes, *Langmuir*, 2009, **26**, 1991-1995.
24 L. A. Sgro, G. Basile, A. C. Barone, A. D`Anna, P. Minutolo, A. Borghese, and A. D`Alessio, *Chemosphere*, 2003, **51**, 1079-1090.
25 H. F. Calcote, D. B. Olson, and D. G. Keil, *Energy & Fuels*, 1988, **2**, 494-504.
26 P. Weilmunster, A. Keller, and K. H. Homann, *Combustion and flame*, 1999, **116**, 62-83.
27 R. A. Dobbins, R. A. Fletcher, and H. C. Chang, *Combustion and flame*, 1998, **115**, 285-298.
28 P. Gerhardt, and K. H. Homann, *J. Phys. Chem.*, 1990, **94**, 5381-5391.
29 N. Gibson, O. Shenderova, T. J. M. Luo, S. Moseenkov, V. Bondar, A. Puzyr, K. Purtov, Z. Fitzgerald, and D. W. Brenner, *Diamond & Related Materials*, 2009, **18**, 620-626.
30 J. Liu, C. H. Liang, Z. F. Tian, S. Y. Zhang, and G. S. Shao, *Scientific Reports*, 2013, **3**, 1741.
31 S. Branko, K. Dragan, and F. Suzana, *Rudarsko-GeoloSko-Naftni Zbornik*, 1992, **4**, 147.
32 L. R. Radovic, and B. Bockrath, *J. Am. Chem. Soc.*, 2005, **127**, 5917-5927.
33 B. Valeur, Molecular Fluorescence: Principles and Applications (WILEY-VCH 2002).